




RESEARCH ARTICLE

Geophysical assessment of Verteba Cave Eneolithic site, Ukraine

Kseniia M. Bondar¹  | Mykhailo P. Sokhatskyi² | Anatolii Chernov¹ |
 Yaroslav Popko¹ | Oleh Petrokushyn¹ | Mariia Baryshnikova¹ |
 Ruslan Khomenko¹ | Myroslav Boyko²

¹Institute of Geology, Taras Shevchenko National University of Kyiv, Kyiv, Ukraine

²Borshchiv Regional Museum of Local Lore, Borshchiv, Ukraine

Correspondence

Kseniia M. Bondar, Institute of Geology, Taras Shevchenko National University of Kyiv, 90 Vasylykivska St, 03022 Kyiv, Ukraine.
 Email: ks_bondar@ukr.net

Scientific editing by Andy Herries

Funding information

Society of Exploration Geophysicists (SEG) Foundation, Grant/Award Number: support of Verteba Geoscience Camp in Ukraine 2018

Abstract

The set of geophysical methods employed above ground and inside Verteba Cave Eneolithic Trypillian Culture Site (Ukraine) includes magnetic survey, electrical resistivity tomography (ERT), and ground-penetrating radar (GPR). The above-ground geophysical study was aimed at the recognition of lateral and vertical distribution of sulfate karst landforms and archaeological targets. In-cave measurements were made to prospect archaeological remains in loose infill and unknown voids. The round and oval-shaped magnetic anomalies with dimensions of 10–25 m and maximum intensity of 15–20 nT are caused by old refilled collapse dolines that were discovered over the cave. The magnetic survey proved the absence of Trypillian culture houses on the surface and the presence of buried archaeological objects in the cave. 2D ERT imaging revealed the vertical structure of karstic collapse dolines, the thickness of the sedimentary layer over gypsum, as well as loamy cave infill. ERT was capable of detecting the void in gypsum by resistivity enhancement up to several thousand ohm-meters. The underground GPR survey of cave walls provided information about possible vertical air–gypsum and loam–gypsum interfaces within the gypsum layer. The prospective areas for future archaeological excavations and the possible location of undiscovered cavities were outlined on the basis of geophysical results.

KEYWORDS

electrical resistivity tomography, Eneolithic, ground-penetrating radar, karst, magnetic survey, Trypillian culture, Verteba Cave

1 | INTRODUCTION

Geophysical methods are widely used in archaeological prospecting (Campana & Piro, 2009; C. Gaffney & Gater, 2003; Gilbert, 2017; Kvamme, 2003). Significant data can be obtained by applying a set of geophysical techniques to reconstruct the spatial structure of the site and geological conditions under which humans lived in the past. An extensive number of research

studies have determined the most informative combination of methods for archaeology, which includes magnetic survey, electrical resistivity, and ground-penetrating radar (GPR; Brizzolari et al., 1992; Cardarelli & Di Filippo, 2009; De Domenico et al., 2006; Di Maio et al., 2016; Drahor, 2006; Drahor et al., 2009; Drahor & Kaya, 2000; V. Gaffney et al., 2004; Keay et al., 2009; Kvamme, 2006; Leucci et al., 2015; Piro et al., 2000; Vermeulen et al., 2006; Welc et al., 2017). These methods have also recently

become an important tool in karst-caves research (Kaufmann et al., 2011; Lazzari et al., 2010; Leucci & De Giorgi, 2005; Mochales et al., 2007; Putis'ka et al., 2014; Welc et al., 2017). Studies describing the application of geophysical methods on karstic terrain emphasize the difficulties due to unfavorable physical properties of the overlying sediments, the presence of water-saturated layers (Lazzari et al., 2010; Prokhorenko et al., 2006), high bedrock surface heterogeneities generated by fractures, and depressions filled with air, soil, and clay material (Cheng et al., 2019; Leucci & De Giorgi, 2005). Being applied together on cave archaeological sites, geophysical methods provide planigraphy as well as stratigraphy of karstic terrain that gives a reliable base to hypothesize on previous uses for the cave.

This paper is devoted to the results of the joint application of the magnetic, electrical resistivity tomography (ERT), and GPR surveys on Verteba Cave in Ukraine. Above-ground and in-cave measurements were performed to understand the karst landform evolution and to determine areas of possible continuation of the cave with archaeological remains from Eneolithic Trypillian culture. The geophysical surveys in the cave also have a goal

to determine promising locations for future archaeological excavations.

1.1 | Location of the study area and geological settings

Verteba Cave is situated at 48°47'N and 25°52'E, north of the Dniester valley, within the Podillia-Bukovynian karst region in Ukraine (Figure 1a). The cave occupies the meander neck of the Seret River (Figure 1b). Geomorphologically, the cave terrain is a sublime (260–310 m) hilly plateau with wide lowlands and shallow watersheds that is limited from the west (3 km from the entrance to the cave) by the valley of the Seret River. The entrance to the cave is located on the steep side of one of the numerous collapse dolines, closed karst depressions formed by a sudden breakdown of the surface above a mechanically unstable underground cavity in the gypsum layer (Jennings, 1985). The cave consists of wide, intertwined galleries, often separated by narrow bridges (Dublianskyi & Lomaev, 1980). Verteba is one of the largest mazes of "The Great



FIGURE 1 Location of Verteba Cave: (a) map of the region, g—Middle Miocene gypsum strata (after Babel, 2005); (b) local topographical map; (c) map of the cave maze, t—part of the maze with Trypillian culture deposits [Color figure can be viewed at wileyonlinelibrary.com]

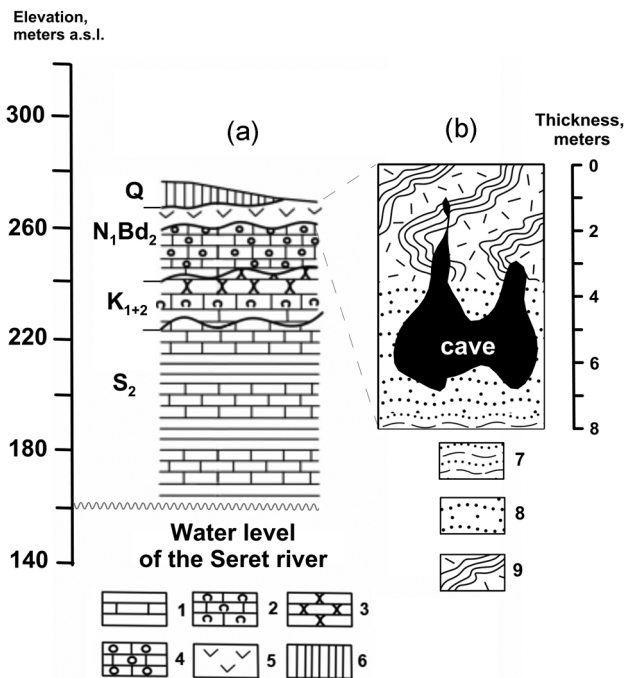


FIGURE 2 Lithostratigraphy of the sedimentary sequence (a) gypsum sequence, (b) hosting Vertebea Cave: (1) clayey dark brown and greenish shales with interlayers of limestone, (2) bryozoan limestone, (3) chalcedonolith, opal-glaucinite, and quartz sand, (4) bank and bioherm red (*Rhodóphyta*) limestone, (5) gypsum, (6) fluvio-glacial loams and gravels, soil, (7) fine-grained or microcrystalline gypsum with relic lamination, (8) fine-grained (alabaster-like) gypsum with traces of gypsified crenulated microbial mats, (9) sabre and megacrystalline gypsum (after Babel, 2005; Dublianskyi & Smolnikov, 1969)

Cave Belt” of the Podillia–Bukovynian karst region. The total length of the studied labyrinth is 9 km (Figure 1c).

The cave is developed in the Middle Miocene (Badenian) gypsum sequence, widespread along the southwestern edge of the Eastern European Platform, in the transition zone between the platform and the Carpathian Foredeep. The gypsum deposits are represented by fine-grained or microcrystalline gypsum with traces of gypsified crenulated microbial mats and relic lamination (lower lithofacies), as well as sabre and megacrystalline gypsum (upper lithofacies; Babel, 2005). In the vicinity of the cave entrance, the gypsum is occasionally exposed at the surface, but typically a 1–3-m thick layer of quaternary loams and gravels covered by topsoil overlies the gypsum. The sulfate bed is underlain by 15–20 m of red (*Rhodóphyta*) limestones of the Lower Badenian age (Figure 2; Dublianskyi & Smolnikov, 1969).

The origin of the cave is controversial. Dublianskyi and Lomaev (1980) assumed Vertebea Cave to be formed in Early–Middle Pleistocene with transit underground flow of the Seret River through the 1.9-km wide neck of the meander. According to these authors, the narrow (100–150 m) karstified area, characteristic orientation, and the morphology of most galleries testify its predominantly erosive origin.

However, Klimchouk (2000) proposed the transverse artesian speleogenetic model that states cave development was due to upward transverse groundwater circulation between the pre-existing subgypsum and supragypsum aquifers (Klimchouk, 1990, 1992, 2000). By the Late Pliocene to Early Pleistocene, the initial erosional entrenchment of Dniester valley established better conditions for discharge and activated the transverse groundwater flow within the artesian system.

1.2 | Archaeology

A unique three-layered settlement of the Trypillian culture was formed during the Eneolithic Age in Vertebea Cave. This is the only large cave, which had been inhabited by a Trypillian population three times. The Vertebea Cave occupies a special place among Trypillian–Cucutenia cultural monuments because there is no analogy of using such a large maze by Eneolithic people.

The cave was discovered in 1820 by Jan Khmeletsky and excavated by Adam Honory Kirkor (1876–1878), Gotfrid Ossovsky (1890–1892), Włodzimierz Demetrykevich (1898–1904, 1907), Kandyba (1929), and Mykhailo Sokhatskyi (1996–2018) (Kadrow & Pokutta, 2016; Sokhatskyi, 2000, 2001, 2012).

A collection of archaeological finds discovered at the end of the 19th century to the beginning of the 20th century is now preserved at the Krakow Archaeological Museum. It contains more than 35,000 ceramic sherds, 300 complete vessels, about 120 whole and fragmented anthropomorphic and zoomorphic clay figures, more than 60 other clay items (spindle whorls and sinkers), about 200 bone and horn items, and 300 flint and stone items, as well as several decorations made of bones and shells.

Since 1995, the expedition of the Borshchiv Local History Museum has carried out comprehensive studies of the cultural layer in the near-surface part of the underground cavity. It conducted a detailed survey of the entire labyrinth and the adjacent area. The remains of 16 Trypillian settlements of stages CI (3700–3200 BC) and CII (3200–2750 BC) were found within a radius of 10 km of the cave. They are synchronous to Vertebea cultural horizons, according to radiocarbon dating of selected materials (3700–2700 BC; Kadrow & Pokutta, 2016; Nikitin et al., 2010). The houses of local Trypillian communities are presented as mass of burnt clay, known in Russian as the “pleshchadka.” Some buildings were workshops for extraction and primary processing of flint. Tools were made not only for their own needs but also for trade. The most attractive places to build settlements were raised areas of relief that were dominant in the surrounding area. No traces of a settlement with traditional Trypillian houses were found near the entrance to Vertebea Cave. This location was unfavorable for settlement due to the lack of water, as the entire area was karstified and actively drained.

The Eneolithic cultural layer in the Vertebea Cave was formed on the natural surface of numerous passages, galleries, and halls as a result of the active and long-lasting use of the underground environment by the Tripillian people (Figure 1c). In general, hydrogenous, gravitational, biogenic, and anthropogenic deposits are

represented in the cave. Hydrogenous clastic deposits are represented by a thick layer of silted loams and chernozem soil material, as well as calcite speleothems formed by infiltrating water. Gravitational clastic deposits include loams, gypsum boulders, and debris on the cave floor. Biogenic deposits contain material from living organisms (guano of bats and animal excrement). A large colony of bats lives in the cave and the near-entrance part of the maze is visited by animals like foxes, martens, and dormice. The anthropogenic deposits include the material remains of human life.

The ceiling of gypsum strata and overlying loamy sedimentary overburden above the cave are thin and highly permeable to soil and surface waters entering the cave through the collapse dolines. Suffosion played the primary role in filling the cavity with clastic loose mechanical deposits. Caverns were constantly silted up through numerous collapse dolines as a result of heavy rains, floods, and sudden melting of snow. Stratigraphy of the deposits indicates that periodic silting in individual passages and halls also occurred during the active use of the cave by the Trypillian people. This is evidenced by the layers of “sterile” loam brought by water. When separate halls and niches were silted up, people did not visit these places for some time, but returned much later. The most extensive insertions of surface loams and chernozem soil material occurred in the post-Trypillian time. However, this process still occurs sporadically today, and in places, passages and wide halls are filled with silt (1.5–2 m thick) almost to the ceiling.

The stratigraphy of the cultural layers could be recognized from Trench 7, excavated in 1996–1998 (Sokhatskyi, 2000), which was laid at a distance of 150 m from the entrance (Figure 1c). The excavation had a loose sediment section with a thickness of up to 2.3 m in situ (Table 1 and Figure 3). Lithologically, the deposits are primarily loamy layers with inclusions of gypsum fragments. Three archaeological

horizons of Trypillian culture (Units 3, 5, 7) are clearly separated by “sterile” layers (Units 4 and 5) that are present in Trench 7. The archaeological horizons belong to the chronological periods of CI and CII and represent three local groups of Trypillian culture.

Some objects discovered during excavations are baked clay beds, the dugouts, fireplaces, and garbage pits. Numerous traces of open hearths are localized throughout the cave used by the Trypillian population. There are white alabaster spots on the gypsum walls, remains of the hearth locations, which are the result of burning. Fireplaces are represented by solid aggregates of ash, quenched pieces of gypsum, coals, and a dense layer of baked clay (Sokhatskyi, 2000, 2001).

2 | MATERIALS AND METHODS

The field measurements were conducted during SEG Geoscience Field Camp that was held from August 20–27, 2018. Figure 4 shows geophysical survey lines and polygons set on the orthophotoplan by measuring coordinates using GPS or a total station.

A magnetic survey is a passive geophysical method utilizing a high sensitivity instrument that measures the Earth's magnetic field strength. Changes in the Earth's magnetic field reflect the varying concentration of magnetic minerals in rocks, soils, and sediments. Archaeological objects and artifacts such as ditches, pits, stone and brick structures, fireplaces, kilns, ceramic vessels, slags, and ferrous metal items cause local field disturbance proportional to magnetization contrast between the object and the adjacent soil or sediment (Aspinall et al., 2008; Fassbinder, 2015; C. Gaffney, 2008; Schmidt, 2002). Field magnetic surveying provides a detailed map that can be used to discriminate geologic and anthropogenic magnetic sources.

TABLE 1 Stratigraphy, Trench 7

Unit	Thickness (m)	Description
1	0.15	Layer of gray-yellowish loam with rough gypsum and limestone debris overlying gypsum rocky bottom
2	0.15–0.2	Coarse-grained lamellated gray loam with gypsum and limestone debris. This is an artificial dip for leveling holes on a rocky bottom
3	0.4–0.6	Dark gray, carbonate loam. Significant concentrations of coals, ashes, and burned gypsum. Contains ceramic shards, flint, and bone products, as well as scattered human and animal bones. The oldest cultural horizon, dated to the late CI phase of Trypillian culture
4	0.1	Pale-yellow loam, carbonate, archaeologically “sterile,” homogeneous
5	0.35–0.4	Mixed layer of dark gray loam containing burned gypsum and charcoal (small remains of burnt wood). Dense saturation with sherds of painted ceramics. Terracotta figurines of humans and animals, bone products (daggers, trowels, amulets) were found. Whole and fragmented mealing stones and animal bones are present. Anthropological materials are in a disturbed condition. Dated to the early CII phase of Trypillian culture
6	0.1–0.2	Pale-yellow loam, carbonate, archaeologically “sterile,” homogeneous
7	0.6	Dark gray lumpy loam with manganese inclusions, small stones, burned lime, and coals. Contains a lot of ceramic shards. Whole small vessels (cups) were found. Gray pottery with cord impressions is prevalent. There are models of sledges, ovens, and spindle whorls among the finds. Dated to the late CII phase of Trypillian culture
8	0.8–1	Chernozem soil material, dark gray, loose, carbonate, with fragments of gypsum and limestone introduced through the collapse doline. Does not contain archaeological finds

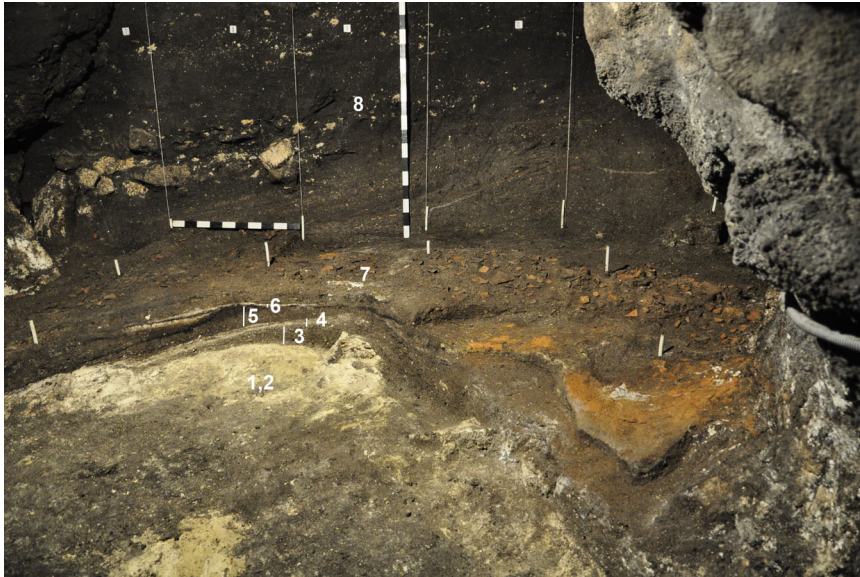


FIGURE 3 Cave deposits in Trench 7. Units are described in Table 1 [Color figure can be viewed at wileyonlinelibrary.com]

The total field magnetometer surveys were performed with a cesium vapor instrument PKM-1M (Geologorazvedka, Russia). This consists of a magnetometer probe with an automatic data logger in a handheld controller.

For the above-ground field survey, the instrument was switched to 10 measurements per second, which gave a spatial resolution of about 10 cm on line. In that mode, the magnetometer had a sensitivity of ± 0.01 nT. A traverse interval was chosen as 1 m. Distance triggering was

performed manually at every line, using start and stop buttons on the controller. Change in the daily variation of the geomagnetic field is reduced to the median value of the 50-m sampling profile and alternatively to the median value of all data of the 50×50 -m grid. The procedure of profile median withdrawal from the measured values allows the exclusion of the normal field (Becker, 1999; Tabbagh, 2003). The difference is then influenced by the target karstic structures and pieces of magnetic rubbish. All measured points were organized in an irregular grid of about

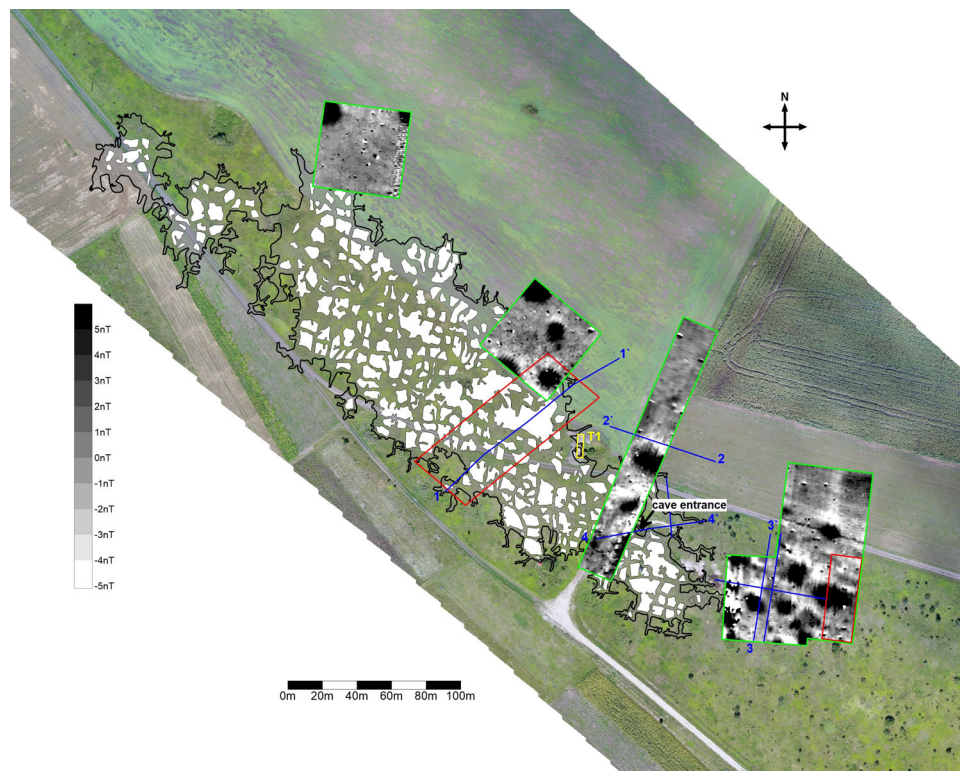


FIGURE 4 Surface magnetic survey grids (green), electrical resistivity tomography lines (blue), ground-penetrating radar grids (red), excavation T1 (yellow), and Verteba Cave map on the orthophotoplan. Magnetic anomaly maps have raster 1.0×0.1 m interpolated to 0.5×0.5 m, intensity of total Earth's magnetic field at the site: $49,560 \pm 25$ nT [Color figure can be viewed at wileyonlinelibrary.com]

0.1 × 1.0 m and transformed (interpolated) to the regular grid of 0.5 × 0.5 m. The magnetic intensity values are represented in a gray scale (Figure 4).

The underground survey was performed in the Archaeological Chamber of the cave in a manual mode. A traverse interval was chosen as 0.5 m. The interval between points on the line was 0.25 m. The ends of each line were geolocated using Leica Disto X310 Laser Distance Meter with an upgrade kit, which adds a three-axis compass and clinometer (Figure 5). We placed another cesium magnetometer unit in the cave to record variations during the survey. The magnetometer was placed in the cave at a 20-m distance from the survey area and operated at the sampling rate of 1 measurement per second. At the processing stage, the variation was subtracted from the measured values along the profile. All measured points were organized in an irregular grid of about 0.25 × 0.5 m and interpolated to the regular grid of 0.12 × 0.12 m. The magnetic intensity values are represented in a gray scale.

GPR is a high-frequency electromagnetic (EM) geophysical technique for surface prospection, which has undergone rapid development during the last decades (Annan, 2003; Daniels, 2004; Finkel'shtein, 1983; Vladov & Starovoitov, 2004).

GPR has been increasingly used in geological, environmental, and archaeological applications due to its high productivity. A GPR device emits EM waves toward the surface of the ground and receives reflected impulses from geological contacts, which separate rocks with different dielectric permittivity and electrical conductivity. With a lower antenna frequency, a larger penetration depth can be achieved, but with a lower resolution.

Prospecting with GPR was carried out with two VIY instruments produced by Transient Technologies LLC, Ukraine, equipped with shielded transmitting antennas with nominal middle frequencies of the emitted EM wave at 125 and 300 MHz. Data were acquired in a continuous mode along survey lines. The data were subsequently processed using standard two-dimensional processing techniques by means of the Synchro3 software (<http://viy.ua/e/software/synchro.htm>). The processing flowchart consists of the following steps: (I) zero-level setting: to determine the depth correctly, it is necessary to match the beginning of the depth scale with a certain point of the direct pulse (e.g., maximum amplitude); (II) dewow operation and wavelet filtering: to suppress effectively low-frequency fluctuations and high-frequency noise; (III) the windowed background removal tool: subtracts an averaged trace from each trace of the profile with the width of the window for averaging specified by the total number of traces; (IV) time gain: to adjust the acquisition gain function and enhance the visibility of deeper anomalies; (V) estimation of the average EM wave velocity by hyperbola fitting. Obtained data were subsequently visualized in various ways to enhance the spatial correlations of anomalies of interest.

ERT is a direct current method where measurements are made through current that is induced into the ground, followed by the registration of resulting potential differences between electrodes placed on a measured line. Different configurations of four electrodes along the line are used to acquire data at different lateral positions along the line. A larger electrode spacing leads to an increase of measurement depth with decreasing resolution.

Seven two-dimensional ERT surveys were carried out across the known cave, as well as at its southeastern periphery, as shown in Figure 4.

Apparent resistivity measurements were acquired using a one-channel device furnished with 64 brass electrodes (Khomenko et al., 2013). All ERT profiles were made using the Schlumberger array protocol. For the surface survey, the electrodes were placed at every 1 m. Such distribution allowed recognition of electrical resistivity readings to a depth of about 11 m. In the cave, the distance between electrodes was 0.25 m, with the maximum depth of 2.5 m.

Measured electrical data were inverted using the interpretation software Res2DINV, employing the robust least-squares optimization technique (L1-norm; De Groot-Hedlin & Constable, 1990; Loke & Barker, 1996; Sasaki, 1992). Bad datum points and points with root mean square (RMS) error higher than 80% were removed from the final inversion. The model was accepted after five iterations or less if a slow convergence rate (<1%) was observed. As the resistivity of soil and fluvioglacial loams and gravels is much lower than the gypsum rock resistivity (Dublianskyi & Smolnikov, 1969) and the loam-gypsum interface could have a complex morphology, the appropriate model with rather high RMS error could be obtained.

3 | RESULTS OF ABOVE-GROUND MEASUREMENTS

3.1 | Magnetic survey results

The total 1.5-ha survey area includes a series of round and oval-shaped magnetic anomalies with dimensions 10–25 m and maximum intensity of 15–20 nT. These anomalies are interpreted as old collapse dolines infilled with topsoil material that are not expressed in the relief (Figure 4).

To estimate how the sediments involved differ by the concentration of magnetic minerals, in situ magnetic susceptibility was measured using KM-7 SatisGeo kappameter in excavation T1, which had opened collapse doline sediments. The topsoil revealed the highest values at $0.6\text{--}0.7 \times 10^{-3}$ SI, whereas underlying loam and gravel strata presented values of $0.2\text{--}0.3 \times 10^{-3}$ SI and gypsum presented diamagnetic negative susceptibility of -0.01×10^{-3} SI.

Soil is characterized by enhanced magnetic susceptibility as compared with underlying loam and gravel layers, and the gravel layers are enhanced more than the underlying sulfate rock (gypsum). Therefore, the collapse of the material from upper to the deeper layers causes the observed positive total field magnetic anomalies over the collapse dolines.

3.2 | ERT results

Sulfate rock, containing between 75% and 100% gypsum, shows electrical resistivity values ranging from 700 to 1000 Ωm (Guinea et al., 2010). According to Dublianskyi and Smolnikov (1969), the Miocene

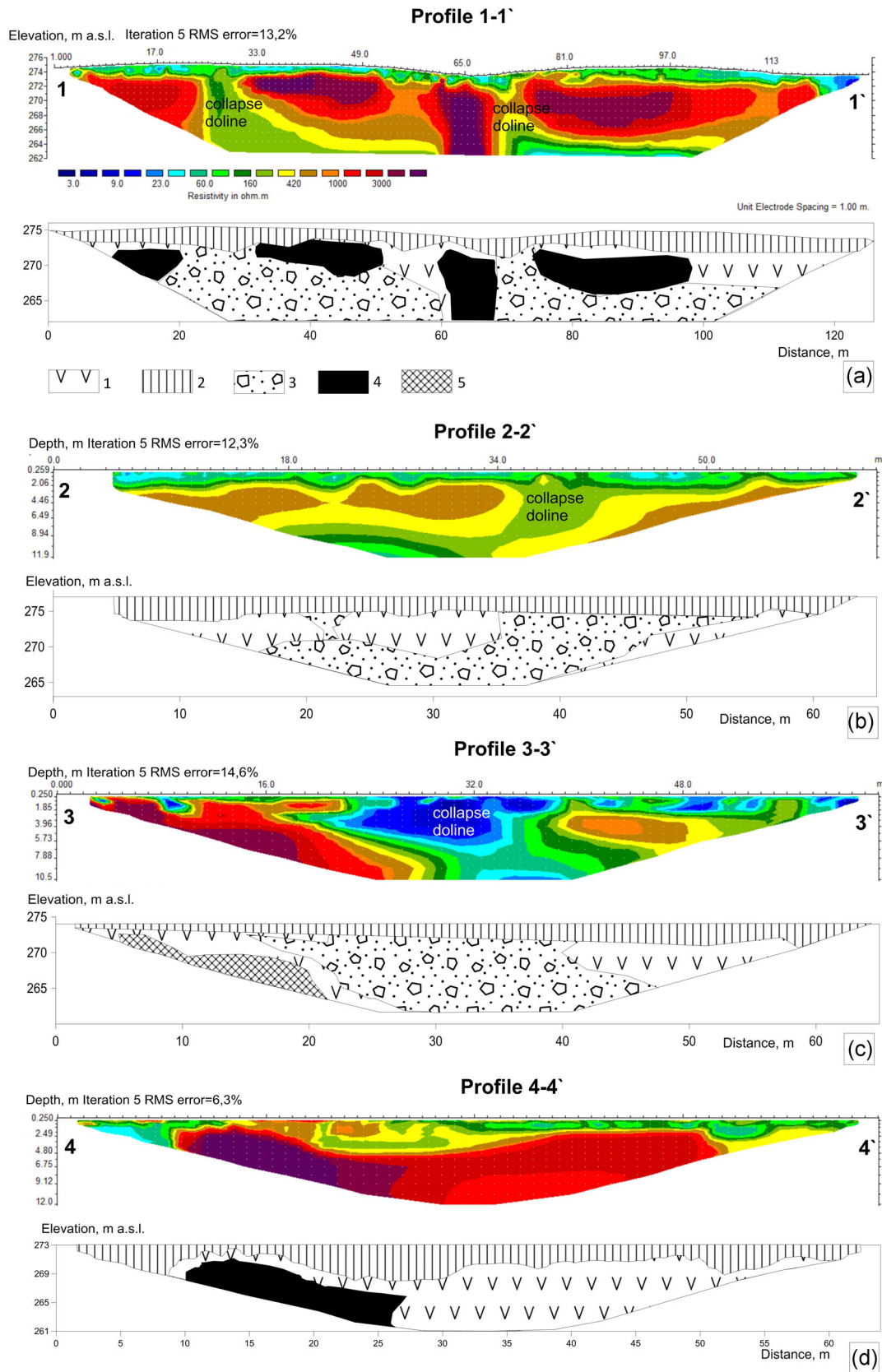


FIGURE 5 Selected above-ground electrical resistivity tomography profiles and their lithological interpretation: (a) profile 1-1'; where (1) gypsum, (2) soil and loam, (3) loamy clastic deposits, (4) cave, (5) predicted cave; (b) profile 2-2'; (c) profile 3-3'; (d) profile 4-4' [Color figure can be viewed at wileyonlinelibrary.com]

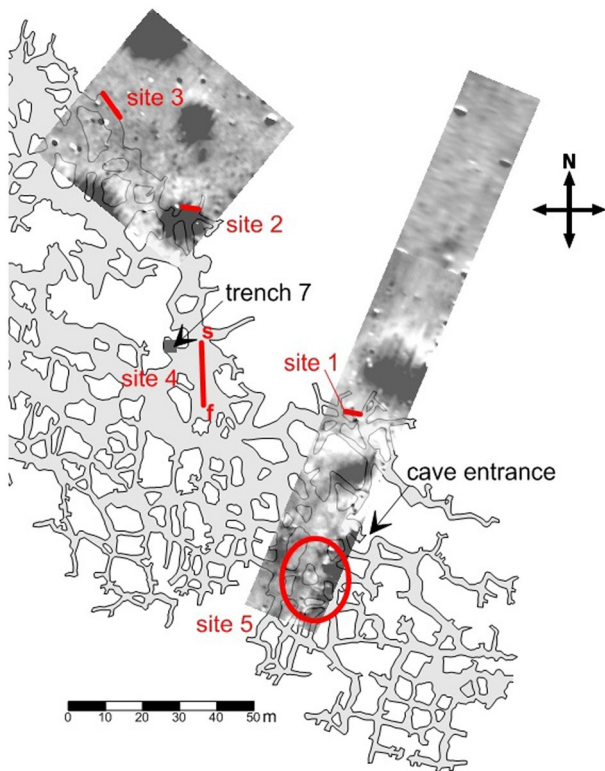


FIGURE 6 Sites in the cave investigated with geophysical methods: (1–3) ground-penetrating radar (GPR) measurements by walls; (4) electrical resistivity tomography and GPR profile by floor; (5) magnetic survey in the Archaeological Chamber [Color figure can be viewed at wileyonlinelibrary.com]

gypsum unit, in which the Verteba Cave is developed (Figure 2), contains over 99% gypsum ($\text{CaSO}_4 \cdot 2\text{H}_2\text{O}$). However, the gypsum layer is not monolithic and its in situ resistivity largely depends on the degree of fracturing and fracture fill.

Geological units, recognized from inverted ERT profiles, are characterized by resistivity values varying from 3 to 6000 Ωm . The gypsum layer is characterized by resistivity close to 1000 Ωm . The presence of cavities filled with air leads to high resistivity values of several thousand ohm-meters. Low resistivity values (<80 Ωm) can be associated with loamy sediments and soils. The intermediate resistivities are due to the sensitivity of the method, which is not capable of distinguishing the sharp interfaces between different layers and heterogeneities within gypsum strata (Figure 6).

Profile 1–1' consisted of three lines of 64 electrodes with 1-m spacing, an overlap of 32 electrodes, and a total length of 128 m. This profile crossed the cave terrain in a NE–SW orientation and topographic correction was taken into account on this profile. The top layer is formed by soil and loam and yields resistivity values <160 Ωm . The bottom layer having lower and higher resistive zones is interpreted as gypsum strata. The values exceeding 2000 Ωm are correlated with the presence of an empty cavity. The lower resistive zones correspond to loamy breakdown material introduced to the cavity through collapse dolines.

Profiles 2–2' and 3–3' reveal the presence of old collapse dolines. The loamy material was incorporated in the gypsum layer, significantly decreasing its resistivity. The ERT interpretation was supplemented by magnetometry results showing the magnetic anomalies associated with the collapse dolines. The gypsum layer with lower resistivity seems to be significantly destroyed by cracks filled with loam and is not likely to host void cave.

The empty cave is interpreted on the Profile 3–3' between 5 and 21 m from the origin of the profile. The gypsum layer is nearly exposed at the surface and the cave is predicted at a depth of 1.3 m.

Profile 4–4' shows the cave in the western portion between 10 and 27 m from the origin of the profile and more or less monolithic gypsum in the eastern portion. There are thin void cracks (0.1–0.3 m) observed on the cave wall of eastward spread from the labyrinth, which are inaccessible to humans but probably caused resistivity enhancement.

3.3 | GPR results

The GPR survey was conducted in two grids over the cave and near it (Figure 4). Georadar antennas of 125 and 300 MHz were used. The soil was identified as chernozem-like with the topsoil with variable thickness of 0.6–1.5 m due to erosion on the slopes of collapse dolines. The average content of clay fraction (<0.005 mm) in the topsoil is 28%–45% (Kit, 2008). Clay produces a high attenuation loss. Therefore, a soil with more than 35% clay effectively adsorbs EM waves, providing poor depth of penetration for GPR exploration (Daniels, 2004). As a result, no information was obtained from surface GPR measurements.

4 | RESULTS OF UNDERGROUND MEASUREMENTS

4.1 | Magnetic survey results

The geomagnetic survey was conducted at the Archaeological Chamber, marked as Site 5 in Figure 7. Considering the magnetic anomaly map represented in Figure 5b, it is necessary to pay attention to the sharp decrease in the geomagnetic field in the northeastern portion of the survey area. The reason for this result is the proximity of the measured survey (about 10 m) to the iron entrance door to the cave, which created the corresponding anomaly.

The chamber contains three features of the probable archaeological origin. The positive anomaly 1 has an intensity of 40 nT. It is about 1 m in size with a round shape. On the northern side, a negative anomaly is observed. Anomalies 2 and 3 have a maximum intensity of 20 and 17 nT, respectively.

4.2 | In-cave GPR and ERT results

Since the Eneolithic Age, the cave passages have experienced silting. The gypsum ceiling collapsed due to the formation of new dolines.

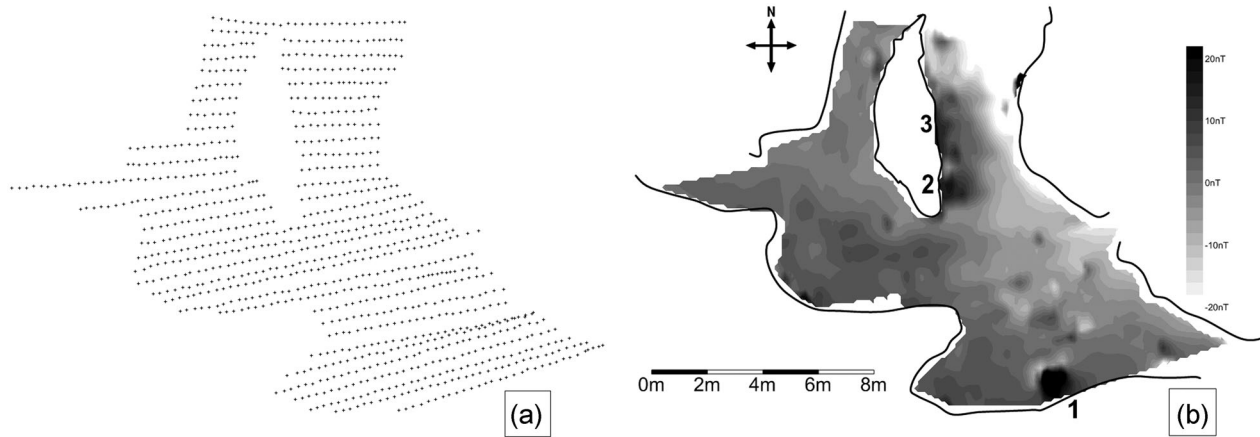


FIGURE 7 Verteba Cave, the Archaeological Chamber. Scheme of magnetic survey points (a) and magnetic anomaly map (b), raster 0.5×0.25 m interpolated to 0.12×0.12 m, the intensity of total Earth's magnetic field at the site: $49,530 \pm 45$ nT

Thus, the parts of cave inhabited by Trypillian people are now inaccessible. Taking into consideration the map of Trypillian cultural layer distribution, we made an attempt to determine whether there are voids to the east of the cave edge by scanning the walls using GPR. The promising results obtained in other gypsum caves of the Podillia–Bukovynian karst region by Prokhorenko et al. (2006) allowed us to expect to find cavities and cracked zones using GPR.

To estimate wave propagation velocity in gypsum and to understand how the gypsum–air border would be visualized, we measured along the gypsum column in the cave with 300-MHz GPR. The gypsum–air interface is visualized rather than a series of diffractions (Figure 8a) with an EM wave velocity of $141 \text{ m}/\mu\text{s}$. To estimate the reflection corresponding to the gypsum–loam interface, we conducted measurements on the ceiling (Figure 8b). This interface has more contrast than in the case of gypsum–air due to the greater difference in the dielectric permittivity between gypsum and loam as compared with gypsum and air (Vladov & Starovojtov, 2004).

Radargram from Site 3 (Figure 7), obtained on the cave wall with a GPR of 125-MHz frequency antenna, revealed a zone of high-amplitude response in the time range of 146–153 ns (Figure 8c). Cavers managed to physically reach the feature indicated on the radargram. It turned out to be a narrow crack, about 0.3–0.5 m wide, which is passable for a human at a distance of about 3 m.

Radargram from the wall at Site 1 presents a signal corresponding to a known passage at a distance of 5 m from the sensing plane (Figure 8d). Behind it, in the range of 175–209 ns (11.7–14 m), another similar zone exists. One can expect a void (cave) in this place. Spatially, it is located near the doline-caused magnetic anomaly.

At Site 2, the gypsum–air interface signal was recorded at the end of the time base of the 300-MHz GPR antenna range. It was also confirmed by the 125-MHz GPR antenna at a distance of 9 m behind the cave wall. We can assume here the presence of a cave (Figure 8e,f).

ERT and GPR sections from Site 4, obtained by 16-m long cave floor profile, yield three layers. The top layer, presented by loamy clastic deposits, has low resistivity. EM wave reflections at 22–25 ns mark the gypsum bottom of the cave. The lower reflections at

40–45 ns could be interpreted as the gypsum–limestone interface, as the bottom layer has enhanced resistivity typical of limestone (Stepišnik & Mihevc, 2008; Telford et al., 1990; Figure 9).

5 | DISCUSSION

The strongest geophysical indicator of terrain affected by karst processes is the presence of magnetic anomalies with a diameter of 10–25 m and an intensity of 15–20 nT. They are mostly round in shape and sourced by collapse dolines. In the cave, they are presented as pouring cones of clastic loams, and on the surface, they exhibit no depression being completely filled with topsoil.

Analyzing the location of magnetic anomalies on the site, we notice them framing the existing maze from the east. This is consistent with the results obtained earlier by Dublianskyi and Smolnikov (1969) regarding the limited size of the karstic zone (strip width: 100–150 m).

The terrain where the visible and refilled collapse dolines are located marks the extent of the former and potential Verteba Cave area (Figure 10). At the same time, the high density of magnetic anomalies observed at the southeastern periphery (area B) indicates a severe deterioration of the gypsum layer, and as a result, the absence of cave in this area. However, in Eneolithic times, some of dolines in area B could have served as entrances to Verteba Cave.

Trypillian population actively used open fire in the cave. This is evidenced by many hearth places on the cave floor and the lamps places on the walls at the intersection of passages, as well as by finding of three baked clay beds (Sokhatskyi, 2000, 2001). We suggest that ventilation of the cave was significantly better than at present due to several entrances in the occupied part of the cave labyrinth. The entrances located at the bottom of collapse dolines have been completely infilled with soil, and the breakdown material was spread through the cave by water. This formed thick layers of loamy cave sediments. Assuming ancient people used the near-entrance part of the cave, areas A and B should be recognized as the most promising places to find archaeological remains.

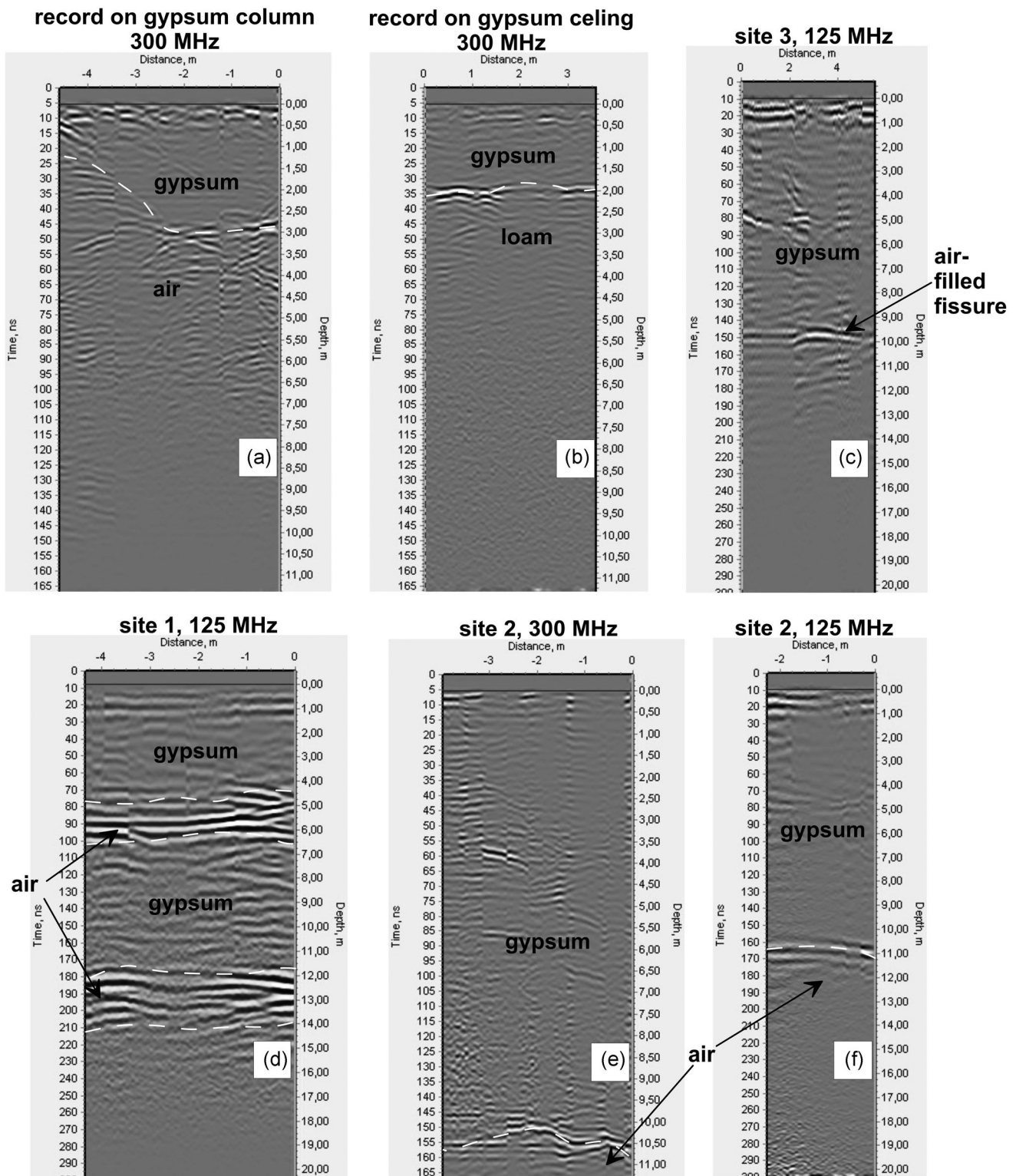


FIGURE 8 Radargrams obtained on the column (a), ceiling (b), and walls (c–f) at the cave at the sites marked in Figure 7

Area A is adjacent to the cave maze at the eastern edge of the cave. It should be considered promising for locating new passages, where according to GPR scans of the walls, vertical boundaries in the gypsum layer are present (Figure 8), especially in cases of the gypsum–air interface. A cavity has been interpreted at Site 2 (Figure 7)

at a distance of about 9 m from the known maze. By excavating the old collapse doline in that area, it would be possible to reach the cultural layer and penetrate into the unexplored part of the maze.

Area B contains small collapsed sinkholes concentrated on the southeastern periphery of Verteba Cave. We hypothesize that it was the

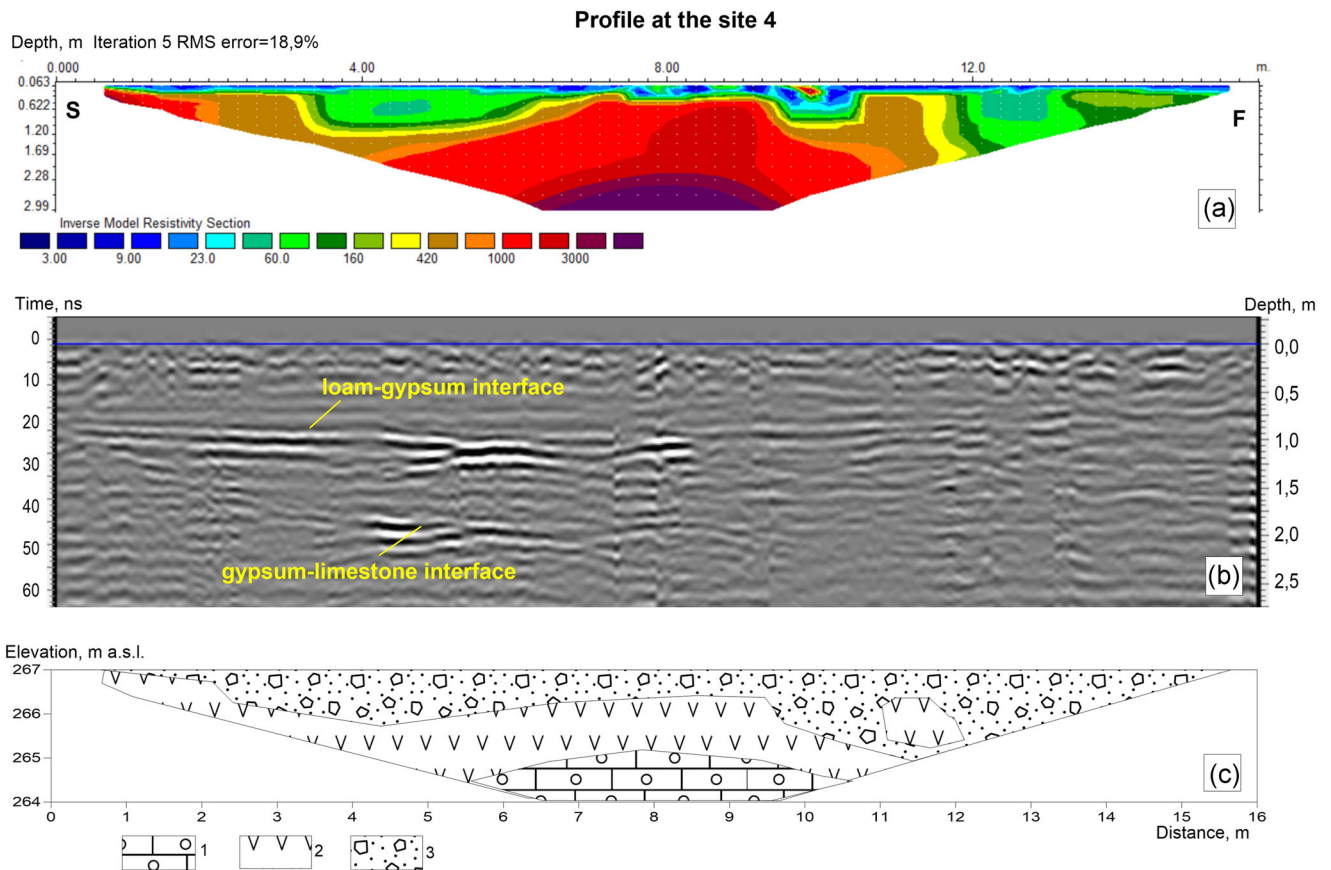


FIGURE 9 Results from Site 4: electrical resistivity tomography profile (a), radargram (b), and their lithological interpretation (c): (1) limestone, (2) gypsum, (3) loamy clastic deposits [Color figure can be viewed at wileyonlinelibrary.com]

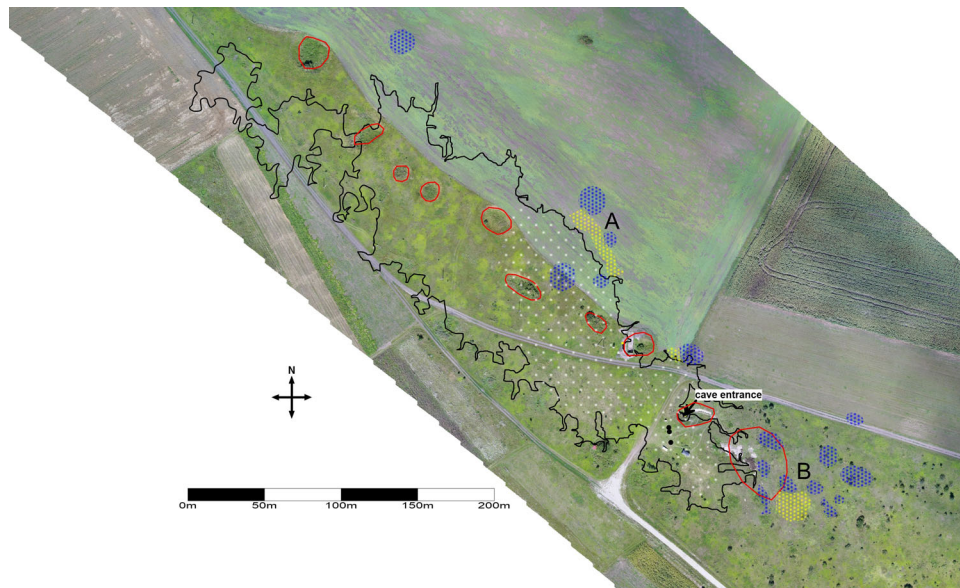


FIGURE 10 A view of the Verteba Cave site with prospective areas for future archaeological study (A and B) in predicted void locations (marked with yellow dots). Collapse dolines interpreted from above-ground magnetic survey are marked with blue dots, and collapse dolines recognized as topographic depressions are outlined in red. The known cave is outlined in black, and the part of the maze with Trypillian culture deposits is marked with white dots. Placement of predicted archaeological objects in the cave is presented with black dots [Color figure can be viewed at wileyonlinelibrary.com]

most favorable part of the cave for Eneolithic human use, and the cultural layers are expected to be buried under the breakdown material. The inverted ERT model shows a void to the west of dolines at a shallow depth of 1.3 m (Profile 3–3' in Figure 5).

An important archaeological result of the surface magnetic survey is that no anomalies have been recorded within the measured grids that can be attributable to Trypillian culture houses or other remnants of habitations from Eneolithic Age. The absence of artifacts of the appropriate time in the plowed topsoil suggests the use of the cave as a cache or a hidden sacred place. Ancient people probably did not live on the surface around the cave.

Underground magnetic measurements in the Archaeological Chamber of the cave revealed anomalies that are recommended for archaeological excavations.

The source of anomaly 1 (Figure 5) could not be reliably assumed, as magnetization, depth, size, and shape of the object are not known. However, having magnetic low on the north, the object most likely could have acquired strong thermal remanent magnetization (TRM) due to burning in-situ. We suggest a baked clay hearth to be the source of anomaly 1. However, it also could be a pit with household pottery sherds or even a single vessel. TRM acquired by baked clay objects on cooling from magnetite/maghemite Curie temperature is very strong and usually many times higher than the initial magnetization of the material. TRM is imparted in the direction of Earth's magnetic field, making an object act as a magnetic dipole, which causes positive anomaly on the south and negative on the north side.

Anomalies 2 and 3 are interpreted as a hearth and a baked clay bed. This makes sense, as three baked clay beds were previously unearthed in the cave (Sokhatskyi, 2001). They were 1.3–0.8-m long, 0.5–0.7-m wide, and 0.3-m thick, consisting of densely packed pottery sherds covered with a layer of baked clay coating. Beds had traces of open fire (charcoals and ashes) on their surface. Obviously, these structures stored heat. It is worth noting that the Trypillian people constructed clay beds in their ground houses. Those remains were found in many settlements (Chernovol, 2008; Shmaglij & Videyko, 1987). Also, clear relief images of beds, located next to the ovens and hearths, can be seen in clay models of Trypillian houses (Kozlov'ska, 1926; Yakubenko, 1999).

ERT and GPR measurements from the cave floor profile at Site 4 (Figure 9) provide information on the depth and geometry of the loam–gypsum interface. Site 4 is located close to Trench 7, where the oldest cultural horizon (Unit 3 in Table 1 and Figure 3) dated to the late CI phase of Trypillian culture lies almost on the gypsum bottom of the cave (Table 1). Thus, the depth of the cultural layer position could be determined by geophysical techniques.

6 | CONCLUSIONS

A combination of total field magnetic survey, GPR, and ERT was used over and inside Verteba Cave with the purpose to specify the geological structure of the karst massif, to identify voids, and to search for archaeological objects in the loamy cave infill.

The magnetic survey proved to be an effective tool to search for old collapse dolines on the currently flat terrain. A total of 16 were recognized by positive round-shaped magnetic anomalies. Together with 10 present sinkholes shown as topographic depressions on the orthophotoplan, they clearly indicate the karstified area.

By means of ERT, we managed to determine the underground structure of the karst massif. We observed high contrast in resistivity values between gypsum rock and loamy material. The geoelectrical sections indicate gypsum as the layer with a significantly higher resistivity ($\approx 1000 \Omega\text{m}$) than the loamy material in the top layer and in collapse dolines, resulting from its considerably smaller primary porosity and fewer interconnected pore spaces. Soil and loam can hold more moisture and have higher concentrations of ions to conduct electricity. Therefore, their resistivity values are below $80 \Omega\text{m}$. ERT was capable of detecting voids in areas behind the cave wall, as demonstrated by resistivity enhancement up to several thousand ohm-meters that is evidenced by correlation ERT results over the known maze. It allowed us to predict the cavity.

No subsurface information was obtained from above-ground GPR measurements with the 125-MHz antenna. The topsoil appeared to be ill-suited to GPR due to the high clay content with high adsorptive capacity for water and exchangeable cations.

Baked clay archaeological objects are predicted by magnetic prospecting in the loamy deposits covering the floor of the Archaeological Chamber of the cave.

ERT and GPR proved to be useful to determine the depth and structure of the loam–gypsum interface, used as a living surface by the Trypillian people.

GPR measurements on cave walls were used to outline air-filled voids. This technique complimented the speleological search for a significant cave that was suitable for human settlement.

Comprehensive analyses of on-ground and underground geophysical results revealed prospective areas and locations for future archaeological excavations.

ACKNOWLEDGMENTS

The authors are exceedingly grateful to the Society of Exploration Geophysicists, SEG Foundation, and TGS for supporting Verteba Geoscience Camp in Ukraine in 2018. They also wish to thank students who participated in the camp and extend special thanks to geodesist Andriy Grachov for his help in data collection. They thank Laurie Whitesell, M.Sc. and the anonymous reviewers for their constructive comments and helpful suggestions, which considerably improved the quality of the manuscript.

CONFLICT OF INTERESTS

The authors declare that there are no conflict of interests.

DATA AVAILABILITY STATEMENT

The data that support the findings of this study are available from the corresponding author upon reasonable request.

ORCID

Kseniia M. Bondar  <https://orcid.org/0000-0002-4946-7707>

REFERENCES

- Annan, A. P. (2003). *Ground penetrating radar principles, procedures and applications*. Sensors and Software.
- Aspinall, A., Gaffney, C. F., & Schmidt, A. (2008). *Magnetometry for archaeologists*. Altamira Press.
- Babel, M. (2005). Event stratigraphy of the Badenian selenite evaporites (Middle Miocene) of the northern Carpathian Foredeep. *Acta Geologica Polonica*, 55(1), 9–29.
- Becker, H. (1999). Duo- and quadro- sensor configuration for high-speed/high-resolution magnetic prospecting with caesium magnetometer. *Archaeological Prospection (Arbeitshefte des Bayerischen Landesamtes für Denkmalpflege)*, 108, 100–105.
- Brizzolari, E., Ermolli, F., Orlando, L., Piro, S., & Versino, L. (1992). Integrated geophysical methods in archaeological surveys. *Journal of Applied Geophysics*, 29, 47–55. [https://doi.org/10.1016/0926-9851\(92\)90012-A](https://doi.org/10.1016/0926-9851(92)90012-A)
- Campana, S., & Piro, S. (Eds.). (2009). *Seeing the unseen. Geophysics and landscape archaeology*. Taylor & Francis Group.
- Cardarelli, E., & Di Filippo, G. (2009). Integrated geophysical methods for the characterization of an archaeological site (Massenzio Basilica Roman forum, Rome, Italy). *Journal of Applied Geophysics*, 68(4), 508–521. <https://doi.org/10.1016/j.jappgeo.2009.02.009>
- Cheng, Q., Chen, X., Tao, M., & Binley, A. (2019). Characterization of karst structures using quasi-3D electrical resistivity tomography. *Environmental Earth Sciences*, 78(2019), 285. <https://doi.org/10.1007/s12665-019-8284-2>
- Chernovol, D. K. (2008). Interior of the Trypillia culture dwellings based on the materials of the settlement of Talyanki. In A. Korvin-Piotrovskiy & F. Menotti (Eds.) *Trypillian culture in Ukraine. The giant settlement Talyanki* (pp. 168–174). Institute of archaeology NASU.
- Daniels, D. J. (2004). *Ground penetrating radar* (2nd ed.). The Institute of Electrical Engineers.
- De Domenico, D., Giannino, F., Leucci, G., & Bottari, C. (2006). Integrated geophysical surveys at the archaeological site of Tindari (Sicily, Italy). *Journal of Archaeological Sciences*, 33(7), 961–970. <https://doi.org/10.1016/j.jas.2005.11.004>
- De Groot-Hedlin, C., & Constable, S. (1990). Occam's inversion to generate smooth, two-dimensional models from magnetotelluric data. *Geophysics*, 55, 1613–1624. <https://doi.org/10.1190/1.1442813>
- Di Maio, R. L. A., Manna, M., & Piegari, E. (2016). 3D reconstruction of buried structures from magnetic, electromagnetic and ERT data: Example from the archaeological site of Phaistos (Crete, Greece). *Archaeological Prospection*, 23, 3–13. <https://doi.org/10.1002/arp.1516>
- Drahor, M. G. (2006). Integrated geophysical studies in the upper part of Sardis archaeological site, Turkey. *Journal of Applied Geophysics*, 59(3), 205–223. <https://doi.org/10.1016/j.jappgeo.2005.10.008>
- Drahor, M. G., Berge, M. A., Oztruk, C., Alpaslan, N., & Ergne, G. (2009). Integrated usage of geophysical prospection techniques in Höyük (tepe, tell)-type archaeological settlements. *ArcheoSciences*, 33, 291–294. <https://doi.org/10.4000/archeosciences.1724>
- Drahor, M. G., & Kaya, M. A. (2000). A large scale geophysical prospection in Achemhöyük, the site of the Assyrian Trade Colony Period. *Turkish Academy of Sciences Journal of Archaeology*, 3, 85–107.
- Dublianskiy, V. N., & Lomaev, A. (1980). *Karst caves of Ukraine* (p. 180). Naukova dumka.
- Dublianskiy, V. N., & Smolnikov, B. N. (1969). *Karstological and geophysical studies of karst cavities in Near-Dniester Podoliya and Pokuttya* (p. 151). Naukova dumka.
- Fassbinder, W. E. (2015). Seeing beneath the farmland, steppe and desert soil: Magnetic prospecting and soil magnetism. *Journal of Archaeological Science*, 56, 85–95. <https://doi.org/10.1016/j.jas.2015.02.023>
- Finkel'shtein, M. I. (1983). *Basics of radar detection*. Radio i Svyaz'.
- Gaffney, C. (2008). Detecting trends in the prediction of the buried past: A review of geophysical techniques in archaeology. *Archaeometry*, 50(2), 313–336. <https://doi.org/10.1111/j.1475-4754.2008.00388.x>
- Gaffney, C., & Gater, J. (2003). *Revealing the buried past: Geophysics for Archaeologists*. Stroud.
- Gaffney, V., Patterson, H., Piro, S., Goodman, D., & Nishimura, Y. (2004). Multimethodological approach to study and characterize Forum Novum (Vescovio, Central Italy). *Archaeological Prospection*, 11, 201–212. <https://doi.org/10.1002/arp.235>
- Gilbert, A. S. (Ed.). (2017). *Encyclopedia of Geoarchaeology*. Springer.
- Guinea, A., Playà, E., Rivero, L., Himi, M., & Bosch, R. (2010). Geoelectrical classification of gypsum rocks. *Surveys in Geophysics*, 31, 557–580. <https://doi.org/10.1007/s10712-010-9107-x>
- Jennings, J. N. (1985). *Karst geomorphology*. Basil Blackwell.
- Kadrow, S., & Pokutta, D. A. (2016). The Vertebe Cave: A subterranean sanctuary of the Cucuteni-Trypillia culture in Western Ukraine. *Journal of Neolithic Archaeology*, 18, 1–21. <https://doi.org/10.12766/jna.2016.1>
- Kaufmann, G., Romanov, D., & Nielbock, R. (2011). Cave detection using multiple geophysical methods: Unicorn cave, Harz Mountains, Germany. *Geophysics* 76(3), B71–B77. <https://doi.org/10.1190/1.3560245>
- Keay, S., Earl, G., Hay, S., Kay, S., Ogden, J., & Strutt, K. D. (2009). The role of integrated geophysical survey methods in the assessment of archaeological landscapes: the case of Portus. *Archaeological Prospection*, 16, 154–166. <https://doi.org/10.1002/arp.358>
- Khomenko, R., Bondar, K., & Popov, S. (2013). New high-resolution shallow-depth multi-electrode equipment for electrical resistivity tomography. *Bulletin of Kyiv University: Geology*, 2(61), 36–40.
- Kit, M. G. (2008). *Soil morphology* (pp. 18–36). Ivan Franko National University of Lviv.
- Klimchouk, A. B. (1990). Artesian genesis of the large maze caves in the Miocene gypsum of the Western Ukraine. *Doklady Akademii Nauk Ukrainskoj SSR*, 7, 28–32.
- Klimchouk, A. B. (1992). Large gypsum caves in the Western Ukraine and their genesis. *Cave Science*, 19, 3–11.
- Klimchouk, A. B. (2000). Speleogenesis of great gypsum mazes in the Western Ukraine. In A. Klimchouk, D. Ford, A. Palmer, & W. Dreybrodt (Eds.), *Speleogenesis: Evolution of karst aquifers* (pp. 261–273). National Speleological Society.
- Kozlov's'ka, V. (1926). Pottery of a culture. In V. Kozlov's'ka (Ed.), *Tripil's'ka kul'tura na Ukraini* (Vol. 1, pp. 139–157).
- Kvamme, K. (2003). Geophysical survey as landscape archaeology. *American Antiquity*, 68, 435–457. <https://doi.org/10.2307/3557103>
- Kvamme, K. (2006). Integrating multi-dimensional geophysical data. *Archaeological Prospection*, 13, 57–72. <https://doi.org/10.1002/arp.268>
- Lazzari, M., Loperte, A., & Perrone, A. (2010). Near surface geophysics techniques and geomorphological approach to reconstruct the hazard cave map in historical and urban areas. *Advances in Geosciences*, 24, 35–44. <https://doi.org/10.5194/adgeo-24-35-2010>
- Leucci, G., & De Giorgi, L. (2005). Integrated geophysical surveys to assess the structural conditions of a karstic cave of archaeological importance. *Natural Hazards and Earth System Sciences*, 5, 17–22. <https://doi.org/10.5194/nhess-5-17-2005>
- Leucci, G., Masini, N., Rizzo, E., Capozzoli, L., De Martino, G., De Giorgi, L., Marzo, C., Roubis, D., & Sogliani, F. (2015). Integrated archaeogeophysical approach for the study of a medieval monastic settlement in Basilicata. *Open Archaeology*, 1, 236–246. <https://doi.org/10.1515/opar-2015-0014>
- Loke, M. H., & Barker, R. D. (1996). Rapid least-squares inversion of apparent resistivity pseudosections by a quasi-Newton method. *Geophysical Prospecting*, 44, 131–152. <https://doi.org/10.1111/j.1365-2478.1996.tb00142.x>
- Mochales, T., Pueyo, E. L., Casas, A. M., & Soriano, M. A. (2007). Magnetic prospecting as an efficient tool for doline detection:

- A case study in the central Ebro Basin (northern Spain). In M. Parise & J. Gunn (Eds.), *Natural and anthropogenic hazards in karst areas: Recognition, analysis and mitigation* (Vol. 279, pp. 73–84). Special Publications.
- Nikitin, A. G., Sokhatsky, M. P., Kovaliukh, M. M., & Videiko, M. Y. (2010). Comprehensive site chronology and ancient mitochondrial DNA analysis from Vertebe Cave—a Trypillian culture site of Eneolithic Ukraine. *Interdisciplinaria Archaeologica: Natural Sciences in Archaeology*, 1(2010), 9–18.
- Piro, S., Mauriello, P., & Cammarano, F. (2000). Quantitative integration of geophysical methods for archaeological prospection. *Archaeological Prospection*, 7, 203–213. [https://doi.org/10.1002/1099-0763\(200012\)7:4<203::AID-ARP133>3.0.CO;2-T](https://doi.org/10.1002/1099-0763(200012)7:4<203::AID-ARP133>3.0.CO;2-T)
- Prokhorenko, V., Ivashchuk, V., Korzun, S., & Stefanyshyn, I. (2006). *Ground penetrating radar survey in Podil'lya karst area (Ternopil Region, Ukraine)*. 11th International Conference on Ground Penetrating Radar, June 19–22, 2006, Columbus, OH.
- Putiška, R., Kušnirák, D., Dostál, I., Lačný, A., Mojzeš, A., Hók, J., Pašteka, R., Krajňák, M., & Bošanský, M. (2014). Integrated geophysical and geological investigations of karst structures in Komberek, Slovakia. *Journal of Cave and Karst Studies*, 76(3), 155–163. <https://doi.org/10.4311/2013ES0112>
- Sasaki, Y. (1992). Resolution of resistivity tomography inferred from numerical simulation. *Geophysical Prospecting*, 40, 453–464.
- Schmidt, A. (2002). *Geophysical data in archaeology: A guide to good practice* (2nd ed.). Oxbow Books.
- Shmaglij, M. M., & Videyko, M. Y. (1987). Late-Trypillian settlement near the village of Maydanetske in Cherkasy region. *Archaeology*, 60, 58–71.
- Sokhatskyi, M. (2000). Excavations of the Borshchiv Local History Museum Archeological Expedition in the Vertebe Cave in 1996–1998. *Litopys Borshschivshchiny*, 9, 3–10.
- Sokhatskyi, M. (2001). Archaeological excavations in the Vertebe Cave at Podolia. In J. Lech & J. Partyka (Eds.), *Z archeologii Ukrainy i Jury Ojcowskiej* (Ojców 2001; pp. 207–227).
- Sokhatskyi, M. (2012). Gotfrid Ossovski—researcher of Trypillian culture in Ternopil region. *Archaeology and Ancient History of Ukraine*, 9, 256–262.
- Stepišnik, U., & Mihevc, A. (2008). Investigation of structure of various surface karst formations in limestone and dolomite bedrock with application of the electrical resistivity imaging. *Acta Carsologica*, 37(1), 133–140.
- Tabbagh, J. (2003). Total field magnetic prospection: Are vertical gradiometer measurements preferable to single sensor survey? *Archaeological Prospection*, 10(2), 75–81. <https://doi.org/10.1002/arp.193>
- Telford, W. M., Geldart, L. P., & Sheriff, R. E. (1990). Resistivity methods. In *Applied Geophysics* (2nd ed., pp. 353–358). Cambridge University Press. <https://doi.org/10.1017/cbo9781139167932.012>
- Vermeulen, F., Hay, S., & Verhoeven, S. (2006). Potentia: An integrated survey of a Roman colony on the Adriatic coast. *Papers of the British School at Rome*, 74, 203–236.
- Vladov, M. L., & Starovoitov, A. V. (2004). *Introduction to georadiolocalization*. MGU.
- Welc, F., Mieszkowski, R., Vrkljan, G. R., & Konestra, A. (2017). An attempt to integration of different geophysical methods (magnetic, GPR and ERT); a case study from the late Roman settlement on the island of Rab in Croatia. *Studia Quaternaria*, 34(1), 47–59. <https://doi.org/10.1515/squa-2017-0004>
- Yakubenko, O. O. (1999). Models of houses from Trypillian collections of the Museum. In N. G. Kovtaniuk (Ed.), *National Museum of History of Ukraine: Its founders and collections: Thematic collection of contributions* (pp. 86–111). Institute of archaeology NASU.

How to cite this article: Bondar KM, Sokhatskyi MP, Chernov A, et al. Geophysical assessment of Vertebe Cave Eneolithic site, Ukraine. *Geoarchaeology*. 2020;1–14. <https://doi.org/10.1002/geo.21827>